Superconductivity near a nematic quantum critical point: Interplay between hot and lukewarm regions

Avraham Klein and Andrey Chubukov

Superconductivity near a nematic quantum critical point – the interplay between hot and lukewarm regions

Avraham Klein and Andrey Chubukov

School of Physics and Astronomy, University of Minnesota, Minneapolis. MN 55455

We present a strong coupling dynamical theory of the superconducting transition in a metal near a QCP towards $Q = 0$ nematic order. We use a fermion-boson model, in which we treat the ratio of effective boson-fermion coupling and the Fermi energy as a small parameter λ. We solve, both analytically and numerically, the linearized Eliashberg equation. Our solution takes into account both strong fluctuations at small momentum transfers $\sim \lambda k_F$ and weaker fluctuations at large momentum transfers. The strong fluctuations determine T_c, which is of order $\lambda^2 E_F$ for both $s-$ and $d-$ wave pairing. The weaker fluctuations determine the angular structure of the superconducting order parameter $F(\theta_k)$ along the Fermi surface, separating between hot and lukewarm regions. In the hot regions $F(\theta_k)$ is largest and approximately constant. Beyond the hot region, whose width is $\theta_h \sim \lambda^{1/3}$, $F(\theta_k)$ drops by a factor $\lambda^{4/3}$. The $s-$ and $d-$ wave states are not degenerate but the relative difference $(T_c^s - T_c^d)/T_c^s \sim \lambda^2$ is small.

Introduction Superconductivity (SC) mediated by fluctuations arising from proximity to an electronic quantum-critical point (QCP) has attracted tremendous interest in the "high T_c" era. Much of the motivation comes from the known proximity of the Cu- and Fe- based superconductors to antiferromagnetism[1–6] but more recent discoveries of charge-density-wave order in the cuprates and of nematic order in both Cu-and Fe-based materials[7–9] have led to studies of SC mediated by critical charge fluctuations[10–12]. Theoretical studies of SC near a QCP show that it is a strong coupling phenomenon, arising from the divergent fluctuations[13–15]. These fluctuations also induce large electronic self-energies, which in the absence of SC would account for a non Fermi liquid (NFL) behavior below some characteristic frequency ω_0[3,13,16–21]. In some systems SC emerges at $T_c \gg \omega_0$ and masks the NFL behavior[15,22], in other systems T_c is smaller than ω_0, at least numerically. In the latter case SC emerges out of a NFL.

A subset of theories of SC in a quantum-critical regime are those dealing with transitions at vanishing momentum transfer $Q = 0$[15–17,21–28]. They are typically associated with a deformation of the Fermi surface (FS) in some angular momentum channel, e.g. $l = 2$ for the nematic transition of the type observed in Fe- and Cu-based SCs. A theory of pairing mediated by soft fluctuations of $d-$wave nematic order parameter must account both for the strong coupling physics that occurs locally on the Fermi surface (FS), and for the momentum anisotropy caused by a $d-$wave form-factor, which occurs on the large momentum scale of the Fermi wavevector k_F.

This paper deals with SC at the nematic QCP. The $\cos 2\theta$ form of the $d-$ wave form-factor splits the FS into four 'hot' regions where $\theta \approx n\pi/2$, $n = 0, 1, 2, 3$, where interactions are strong, and four 'lukewarm' regions where $\theta \approx (n + 1/2)\pi/2$, where the pairing interaction is much weaker[29,30]. Previous studies of this problem have focused either on the pairing away from a QCP within a Fermi liquid framework [29], or on local strong-coupling properties in the hot regions[14,15,22,31,32], where the in-

teraction is at its maximum, but doesn't distinguish between pairing channels. These studies found that T_c is comparable to the upper boundary of the NFL behavior. The weak coupling FL study focused on the angular variation of the gap along the whole FS and on the difference between the pairing strength in different spin-singlet pairing channels. This study found that at a finite distance from a nematic transition (measured by the inverse correlation length ξ^{-1} of nematic fluctuations) $s-$ wave pairing wins over $d-$ wave and higher symmetry channels, but the splitting between the coupling strength in different channels scales as ξ^{-1} and vanishes at a QCP. That work also found that, at a finite ξ^{-1}, there are two scales in the problem: the relevant momentum transfer in the gap equation is of order ξ^{-1}, but the gap varies at a larger scale $\xi^{-1/3}$. In the FL description, both scales collapse when ξ diverges.

Our work unifies the strong coupling and weak coupling approaches. We analyze the pairing near a $Q = 0$ nematic QCP including both the angular dependence of the nematic form-factor along the FS and the dynamics of the pairing interaction and associated self-energy $\Sigma(\theta, \omega_m)$. We obtain T_c in different pairing channels and the angular variation of the pairing gap by solving the linearized Eliashberg gap equation right at a QCP, where $\xi^{-1} = 0$. We argue that the gap variation along the FS and the difference between the couplings in $s-$wave and $d-$wave channels are governed by a single dimensionless parameter λ, which is the ratio of the effective boson-fermion coupling and the Fermi energy, which we assume to be of order bandwidth. At a metallic QCP, interaction is assumed to be smaller than the bandwidth, and we treat λ as a small parameter.

We show that T_c remains finite at a QCP, and $s-$wave and $d-$wave channels remain non-degenerate. The difference between the two comes from the dynamical part of the pairing interaction. The T_c for $s-$wave pairing is higher, and the difference $1 - T_c^d/T_c^s \propto \lambda^2$. We show that the angular dependence of the form-factor causes a sharp angular variation of the pairing gap along the FS in

both $s-$ and $d-$channels as a function of distance θ along the FS from where the form factor is maximal (i.e., from $\theta = n\pi/2$). The pairing gap is the largest in "hot" regions with a width of order $\theta_h \sim \lambda^{1/3}$. This scale is parametrically larger than the typical momentum transfer by the interaction, $O(\lambda)$, but smaller than typical scale of variation of the form-factor, which is $\theta = O(1)$. Between the two scales the gap behaves as $(\theta_h/\theta)^4$. This behavior holds for both $s-$ wave and $d-$ wave pairing gaps, and the difference between the two develops at $\theta = O(1)$.

The Model. We base our study on the standard boson-fermion coupling model[16,33,34]. The bosons represent some collective degree of freedom, either charge excitations near a Pomeranchuk instability, or some composite spin fluctuations responsible for d-wave nematic order. We assume a circular FS and dispersion $\epsilon_{\mathbf{k}} = k^2/2m - \mu$, but a generalization to a more general FS is straightforward. The $d-$wave symmetry of a nematic order is encoded in the fermion-boson interaction,

$$H_I = g \sum_{\mathbf{q},\mathbf{k},\sigma} f(\mathbf{k})\phi(\mathbf{q})\psi_\sigma^\dagger \left(\mathbf{k} + \frac{\mathbf{q}}{2}\right)\psi_\sigma\left(\mathbf{k} - \frac{\mathbf{q}}{2}\right), \quad (1)$$

in which $f(\mathbf{k})$ represents the $d-$wave form-factor and $\phi(q)$ is a bosonic field with static propagator $\chi(q) = \chi_0/(q^2 + \xi^{-2})$. At a QCP, $\xi^{-2} = 0$. The effective boson-fermion interaction is $\bar{g} = g^2\chi_0$ and the dimensionless coupling $\lambda \sim \bar{g}/E_F$. In our problem, the relevant degrees of freedom are near the FS, so we approximate $f(\mathbf{k})$ by an angular function $f(\theta_k) = \cos 2\theta_k$.

We use as an input the result of earlier studies[3,17,35–37] that to leading order in λ fermionic and bosonic self-energies are given by one-loop expressions with free-fermion propagators. The bosonic self-energy gives rise to Landau damping and changes the bosonic propagator at a QCP to

$$\chi(q,\theta_q,\Omega_m)^{-1} \approx \chi_0^{-1}\left(q^2 + \gamma f^2(\theta_q)\frac{|\Omega_m|}{v_F q}\right), \quad (2)$$

where $\gamma = \bar{g}m/\pi$ and $\bar{g} = \chi_0 g^2$ is the effective coupling. For fermions at the FS, the momentum transfer is $q = 2k_F \sin\theta_q/2$, and the susceptibility becomes the function of only θ_q and Ω. The fermionic self-energy near the FS is

$$\Sigma(\theta_k,\omega_m) = \omega_0^{1/3}|f(\theta_k)|^{4/3}|\omega_m|^{2/3}\text{sgn}\omega_m \quad (3)$$

where $\omega_0 = (\bar{g}/2\pi\sqrt{3})^3/\gamma v_F^2 \sim \bar{g}^2/E_F \sim \lambda^2 E_F$. The $\omega^{2/3}$ form is a result of the $z = 3$ scaling.

   a. **The Eliashberg equation.** In order to obtain the linearized Eliashberg equation for the anomalous pair function $F(\theta_k,\omega_n)$ we consider the ladder series of diagrams for infinitesimally small $F(\theta_k,\omega_n)$ with $g^2\chi(q,\theta_q,\Omega_m)$ as the interaction and use full fermionic propagators with the self-energy $\Sigma(\theta_k,\omega_m)$. The Eliashberg equation is obtained by approximating the pairing interaction by that for fermions right on the FS (i.e., approximating $\chi(q,\theta_q,\Omega_m)$ by $\chi(\theta_q,\Omega_m)$ and integrating
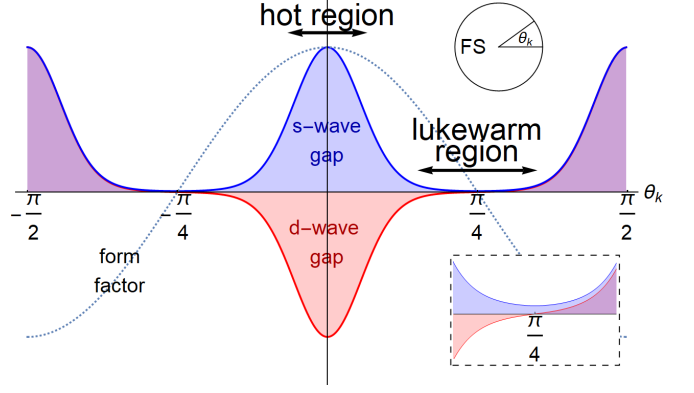

FIG. 1. (color online) Behavior of the gap around the Fermi surface. The image depicts the numerical solution of the linearized Eliashberg gap equation (4) at a nematic QCP, with the interaction form-factor $f(\theta_k) = \cos 2\theta_k$ (dashed line). The blue (dark) and red (light) filled curves depict $s-$ wave and $d-$ wave solutions of the gap equation for weak coupling $\lambda = 0.025$. In both cases, the gap function is maximized in "hot" regions near $\theta = n\pi/2$, where the attraction is maximal. The width of a hot region is of order $\lambda^{1/3}$. Outside, the gap function rapidly drops and becomes of order $\lambda^{4/3}$, creating a "lukewarm" region (inset).

out the momentum transverse to the FS in the fermionic propagators. This is justified because typical bosonic momenta $q \sim \omega^{1/3}$ are parametrically larger than typical fermionic momenta $|k - k_F| \sim \Sigma/v_F \sim \omega^{2/3}$ for $\omega < \omega_0$ and $|k - k_F| \sim \omega/v_F$ for $\omega > \omega_0$. Integrating over the momentum transverse to the FS we obtain

$$F(\theta_k,\omega_n) = \lambda T \sum_{\omega_m \neq \omega_n} \int_{-\pi}^{\pi} \frac{d\theta_q}{2\pi} \frac{F(\theta_k + \theta_q, \omega_m)}{|\omega_m + \Sigma(\theta_k + \theta_q, \omega_m)|} \times$$
$$\frac{|2\sin\theta_q/2| f^2(\theta_k + \theta_q/2)}{|2\sin\theta_q/2|^3 + \frac{\gamma|\omega_n - \omega_m|}{k_F^3 v_F}f^2(\theta_k + \theta_q/2)} \quad (4)$$

where we defined explicitly

$$\lambda = \frac{\bar{g}m}{2k_F^2} = \frac{\bar{g}}{4E_F}, \quad E_F = \frac{k_F v_F}{2}. \quad (5)$$

Notice that this is a 2D integral equation in both frequency and the angle along the FS. We removed the thermal contribution $\omega_n = \omega_m$, as it does not affect T_c for spin-singlet pairing[13,38,39], similar to the effect to non-magnetic impurities[40,41]. Note that because $\Sigma(\theta_k,\omega_m) \propto \omega_m(\omega_0/\omega_m)^{1/3}$ and $\gamma|\omega_n - \omega_m|/(k_F^3 v_F) \propto \lambda^3|\omega_n - \omega_m|/\omega_0$, Eq. (4) depends on a single parameter λ, when T is rescaled by ω_0.

Eq. (4) has a straightforward interpretation. The $F/|\omega + \Sigma|$ term is the result of integrating out the fermionic particle-particle bubble, that for a constant interaction would give the usual $F/|\omega_m|$ BCS form of the gap equation. The term on the second line is the bosonic susceptibility, weighted by the vertex form-factors, and $2k_F\sin(\theta_q/2)$ is momentum variation between two points

on the FS separated by an angle θ_q. For small angles, $2\sin(\theta_q/2) \approx \theta_q$. Because of f^2- factor in various places in the Eliashberg equation, the FS can be segmented into 'hot' regions, where $f^2(\theta) \simeq 1$, and 'lukewarm' regions where $f^2(\theta) \ll 1$. Fig. 1 depicts the behavior of the form-factor and shows the hot and lukewarm regions of the FS.

b. T_c and the angular variation of $F(\theta_k, \omega_m)$. We first obtain T_c. The frequency sum over ω_m in (4) is UV convergent, hence typical ω_n and ω_m are of the same order of T_c Typical θ_q are then of order $(\gamma|\omega_n - \omega_m|)^{1/3} \sim \lambda(T_c/\omega_0)^{1/3}$. We will see that in our case $T_c \sim \omega_0$. Then typical θ_q are of order $\lambda \ll 1$. The $d-$wave form-factor does not vary on such scale and can be set to $f = 1$. We assume and then verify that $F(\theta_q + \theta_k, \omega_m)$ also varies slowly at $\theta_q = O(\lambda)$ and can be approximated by $F(\theta_k, \omega_m)$. In this situation we can integrate over θ_q in (4) and obtain a local gap equation,

$$F(\theta_k, n) \approx \sum_{m \neq n} F(\theta_k, m)\Lambda(m, n), \qquad (6)$$

where

$$\Lambda(m, n) = \frac{1}{3} \frac{1}{\left|m + \frac{1}{2}\right|^{2/3} |m - n|^{1/3}} \frac{1}{1 + \left|2\pi T(m + \frac{1}{2})/\omega_0\right|^{1/3}} \qquad (7)$$

Eq. (6) is dimensionless, local, and universal in the sense that dimensionless λ cancels out. Solving Eq. (6) numerically, we find

$$2\pi T_c = 2.9\omega_0 = 3.5 \times 10^{-3} \frac{\bar{g}^2}{E_F}. \qquad (8)$$

This is consistent[42] with earlier works[14,21,23,32,43].

We next look at a lukewarm region and examine whether the interaction within this region can give rise to a comparable T_c. For definiteness let's focus on θ_k near $\pi/4$. In lukewarm regions we need to differentiate between s-wave and $d-$wave (even and odd) solutions with $F^s(\theta_k, \omega_n) \approx F^s(\pi/4, \omega_n)$, $F^d(\theta_k, \omega_n) \approx F^d(\omega_n)\delta\theta_k$, where $\delta\theta_k = \theta_k - \pi/4$. Because $f^2(\pi/4 + \theta_q/2) = \sin^2\theta_q/2$, the effective static boson-mediated interaction $f^2(\pi/4 + \theta_q/2)\chi(\pi/4 + \theta_q/2) = \bar{g}/(4k_F^2) = \lambda(2m)$ is not singular and weak. In this situation, one can neglect both the Landau damping and the fermionic self-energy. Then $F^s(\pi/4, \omega_n)$ does not depend on ω_n, i.e., the pairing is described by BCS theory, with an onset temperature $T_s^{luke} \propto e^{-1/\lambda_s}$, where $\lambda_s = O(\lambda)$. The temperature T_s^{luke} is indeed much smaller than T_c in Eq. (8), and the same holds for d-wave pairing. This implies that s-wave SC in a lukward region is induced by that in the hot regions.

We now determine the angular variation of the gap in the hot regions. For definiteness consider the segment $0 \leq 0 \leq \pi/4$. We label a characteristic θ at which $F(\theta_k, \omega_n)$ varies as θ_h. At a first glance, θ_h should be of order one because $f(\theta)$ varies at $\theta = O(1)$. However, we show that θ_h is actually parametrically smaller and

is of order $\lambda^{1/3}$. To see this, we assume that $\theta_h \ll 1$ and then verify it. Because typical ω_m and ω_n in the Eliashberg equation are of order T_c, i.e., $\omega_n \sim T_c$ and $\gamma|\omega_m - \omega_n|/k_F^3 v_F \sim \lambda^3$, we can reduce the 2D integral equation (4) to a 1D equation on θ_k:

$$F(\theta_k) = \frac{3\sqrt{3}\lambda}{4} \int \frac{d\theta_q}{\pi} \frac{F(\theta_k + \theta_q)|\theta_q|}{|\theta_q|^3 + \lambda^3} f^2\left(\theta_k + \frac{\theta_q}{2}\right). \qquad (9)$$

If we approximate $f^2(\theta_k + \theta_q/2)$ by 1 and $F(\theta_k)$ and $F(\theta_k + \theta_q)$ by $F(0)$, we see that Eq. (9) reduces to an identity, as should be for $T = T_c$. Going beyond this approximation, we expand $f^2(\theta_k + \theta_q/2)$ in (9) as $1 - (\theta_k + \theta_q/2)^2/2$. For $\theta_k < \theta_h$ the second term in f^2 is irrelevant by construction, but for $\theta_h \leq \theta_k \ll 1$ it plays a major role. Indeed, for these θ_k there are two contributions to the r.h.s. of (9). One comes from the integration over a narrow range $\theta_q \sim \lambda$ and yields $F(\theta_k)(1 - O(\theta_k^2))$. The other comes from the coupling to hot region, where $F(\theta_k + \theta_q) \approx F(0)$. Typical θ_q for this second contribution are $\theta_q \sim -\theta_k$, i.e., they are parametrically larger than λ. This second contribution is then of order $\lambda F(0)\theta_h/\theta_k^2$. Substituting the sum of the two contributions into the r.h.s. of (9) we obtain

$$F(\theta_k) \sim F(0)\lambda \frac{\theta_h}{\theta_k^4} \qquad (10)$$

By construction, $F(\theta_k)$ is supposed to vary at $\theta_k \sim \theta_h$. This yields $\lambda\theta_h \sim \theta_h^4$, i.e.,

$$\theta_h \sim \lambda^{1/3}. \qquad (11)$$

This scale is in between the "width" of the interaction λ and $\theta = O(1)$, at which $f(\theta)$ evolves. We see from (10) that at $\theta_h \leq \theta_k \ll 1$, $F(\theta_k) \sim F(0)(\theta_h/\theta_k)^4$. At $\theta_k = O(1)$ (in the lukewarm region) $F(\theta_k) \sim F(0)\theta_h^4 \sim F(0)\lambda^{4/3} \ll F(0)$. The behavior of $F(\theta_k)$ in this region is different for $s-$wave and $d-$wave pairing (see below). In Fig. 2 we show the result of the numerical solution of the full 2D Eliashberg equation (4). We see that for the full dynamical problem both the width of the interaction, and the width of the gap, are finite at a QCP. This is in contrast to a FL analysis[29], where both vanish as $\xi^{-1}, \xi^{-1/3}$ respectively, at a QCP.

c. $s-$wave vs $d-$wave pairing symmetry To obtain the global structure of the gap function and determine the splitting of onset temperatures T_c^s, T_c^d for $s-$wave vs $d-$ wave pairing, we need to take into account variations of the gap function over large regions of the FS, $|\theta_q| \sim \pi/2$. Naively, we expect $s-$ and $d-$ wave splitting to be determined by whether the nematic attraction prefers a nodal d-wave structure or non-nodal $s-$wave structure. However, it turns out that the condensation energy from $d-$wave nodes is of order $\lambda^{11/3}$, and is much smaller than the actual $s - d$ energy difference which is of order λ^2. Instead, the splitting originates from the difference in the interactions between hot regions. To show this, we again reduce the 2D integral equation (4) to the
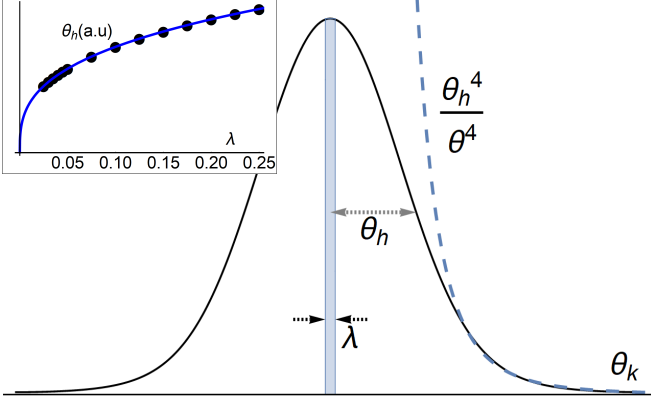
FIG. 2. Numerical solution of the full Eliashberg equation, Eq. (4), at small deviations from $\theta_p = 0$. Main panel – the gap function for $\lambda = 0.025$. We define $2\theta_h$ as the full width at half-maximum. Insert – the dependence of θ_h on λ. The solid line is a fit to $\lambda^{1/3}$. At $\theta > \theta_h$, the gap function scales as $(\theta_h/\theta)^4$, in agreement with Eq. (10).

effective 1D equation on θ_k, as in Eq. (9), but now do not expand the r.h.s. in small θ_k and θ_q. The full effective 1D equation differs from (9), and this difference can be modeled by introducing eigenvalues $\eta_{s,d} \neq 1$, different for $s-$wave and $d-$wave pairing. Setting $\theta_k = 0$, we then obtain

$$\eta_{s,d}F(0) = \frac{3\sqrt{3}\lambda}{4} \int \frac{d\theta_q}{\pi} \frac{F(\theta_q)|2\sin\theta_q/2|}{|2\sin\theta_q/2|^3 + \lambda^3} f^2\left(\frac{\theta_q}{2}\right). \tag{12}$$

One can verify that larger eigenvalue corresponds to larger T_c. Our goal is to find $\eta_s - \eta_d$.

The leading contribution to the r.h.s. of (12) comes from $\theta_q \leq \lambda$. This leading term, however, does not differentiate between $s-$wave and $d-$wave pairings. The one which differentiates between the two comes from the range of order θ_h near $|\theta_q| = \pi/2$. This contribution is of order $\lambda\theta_h^3 \sim \lambda^2$ (the additional θ_h^2 is due to $f^2(\theta_q/2) \propto \theta_h^2$ in the region $\theta_q \sim \pm\pi/2$). Accordingly, the splitting between $s-$wave and $d-$wave couplings is

$$\eta_s - \eta_d \sim \lambda^2 \sim \frac{\omega_0}{E_F} \sim \frac{T_c}{E_F}. \tag{13}$$

The eigenvalue splitting gives rise to the splitting between T_c^s and T_c^d: $(T_c^s - T_c^d)/T_c^s \sim \eta_s - \eta_d \propto \lambda^2$ (i.e., $T_c^s - T_c^d \propto E_F\lambda^4$). One can verify that the higher eigenvalue is η_s, as one expects considering that the interaction is purely attractive. We also verified Eq. (13) by numerically solving Eq. (4)[44].

Eqs. (8) and (13) portray the interplay between long- and short- scales near a QCP. The divergence of static fluctuations near the QCP is cut off by the boson dynamics, setting the IR scale of momentum transfer $\theta_q \sim \lambda$. Interactions at this scale provide the largest contribution, of order $\omega_0 \sim \lambda^2 E_F$, to T_c in both $s-$wave and $d-$wave channels. The degeneracy between T_c in the two channels
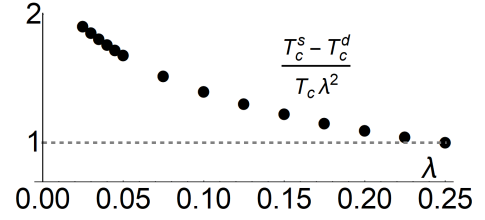

FIG. 3. The splitting of T_c^s and T_c^d as a function of λ from the solution of the full 2D Eliashberg equation. We plot the ratio $(T_c^s - T_c^d)/(T_c^s\lambda^2)$, normalized to 1 at $\lambda = 0.25$. The result agrees with Eq. (13).

is lifted by the much weaker interaction at large momentum transfer of $\theta_q \sim 1$, and has additional smallness in λ^2. Note that although $\eta_s - \eta_d \propto \lambda^2$, the the effective 1D equation (12), from which we extracted $\eta_s - \eta_d$, neglects self-energies at large angles, so we don't need to compute self-energies to order λ^2.

d. **Summary.** In this communication we studied strong coupling theory of SC in a metal near a QCP towards $q = 0$ nematic order. We used fermion-boson model, and treated the ratio of effective boson-fermion coupling and the Fermi energy as a small parameter λ. We solved the linearized Eliashberg equation and verified that T_c is finite at a QCP and is of order $\lambda^2 E_F$ for both $s-$wave and $d-$wave pairing. The two are not degenerate and T_c^s is larger than T_c^d, but the difference $T_c^s - T_c^d \sim \lambda^4 E_F$ is much smaller than each of these temperatures. We also analyzed angular variation of the superconducting order parameter $F(\theta_k)$ along the FS. We showed that $F(\theta_k)$ is the largest in hot regions on the FS, whose width $\theta_h \sim \lambda^{1/3}$. Within a hot region (at $\theta_k < \theta_h$), the order parameter is approximately a constant. Outside, it drops as $(\theta_h/\theta_k)^4$ and becomes smaller by a factor $\lambda^{4/3}$. This behavior holds for both $s-$wave and $d-$wave order parameters. The two become different only at $\theta_k = O(1)$.

We end with a word of caution. In this work we considered $F(\theta_k)$ which monotonically decreases between hot and lukewarm regions and does not change sign along the arc $0 < \theta_k < \pi/4$. There exist other $s-$wave and $d-$wave solutions of Eq. (4), which change sign $n \geq 1$ times. These additional solutions emerge at smaller T and do not affect T_c^s, T_c^d, and the structure of $F(\theta_k)$ near T_c in each channel. Still, if T_c for these additional solutions of the linearized equation is small compared to T_c only by some power of λ, we expect that the form of $F(\theta_k)$ near $T = 0$ will be quite different from that near T_c.

---

[1] H. v. Löhneysen, A. Rosch, M. Vojta, and P. Wölfle, Rev. Mod. Phys. **79**, 1015 (2007).

[2] P. Monthoux, D. Pines, and G. G. Lonzarich, Nature **450**, 1177 (2007).

[3] A. Abanov, A. V. Chubukov, and J. Schmalian, Advances in Physics **52**, 119 (2003).

[4] D. J. Scalapino, Rev. Mod. Phys. **84**, 1383 (2012).

[5] S. Sachdev, M. A. Metlitski, and M. Punk, Journal of Physics: Condensed Matter **24**, 294205 (2012), and references therein.

[6] O. Cyr-Choinière, R. Daou, F. Laliberté, C. Collignon, S. Badoux, D. LeBoeuf, J. Chang, B. J. Ramshaw, D. A. Bonn, W. N. Hardy, R. Liang, J.-Q. Yan, J.-G. Cheng, J.-S. Zhou, J. B. Goodenough, S. Pyon, T. Takayama, H. Takagi, N. Doiron-Leyraud, and L. Taillefer, Phys. Rev. B **97**, 064502 (2018).

[7] L. Taillefer, Annu. Rev. Condens. Matter Phys. **1**, 51 (2010).

[8] T. Shibauchi, A. Carrington, and Y. Matsuda, Annu. Rev. Condens. Matter Phys. **5**, 113 (2014).

[9] A. Coldea and M. Watson, ArXiv:1706.00338.

[10] R. M. Fernandes, A. V. Chubukov, and J. Schmalian, Nat Phys **10**, 97 (2014).

[11] F. Wang, S. A. Kivelson, and D.-H. Lee, Nat Phys **11**, 959 (2015).

[12] Y. Wang and A. Chubukov, Phys. Rev. B **90**, 035149 (2014).

[13] A. Abanov, A. V. Chubukov, and A. M. Finkel'stein, EPL (Europhysics Letters) **54**, 488 (2001).

[14] Y. Wang, A. Abanov, B. L. Altshuler, E. A. Yuzbashyan, and A. V. Chubukov, Phys. Rev. Lett. **117**, 157001 (2016).

[15] S. Raghu, G. Torroba, and H. Wang, Phys. Rev. B **92**, 205104 (2015).

[16] B. L. Altshuler, L. B. Ioffe, and A. J. Millis, Phys. Rev. B **50**, 14048 (1994).

[17] M. A. Metlitski and S. Sachdev, Phys. Rev. B **82**, 075127 (2010).

[18] M. A. Metlitski and S. Sachdev, Phys. Rev. B **82**, 075128 (2010).

[19] M. A. Metlitski and S. Sachdev, New Journal of Physics **12**, 105007 (2010).

[20] S. Lederer, Y. Schattner, E. Berg, and S. A. Kivelson, Proc Natl Acad Sci USA , (2017).

[21] S.-S. Lee, Annu. Rev. Condens. Matter Phys. **9**, 227 (2018).

[22] M. A. Metlitski, D. F. Mross, S. Sachdev, and T. Senthil, Phys. Rev. B **91**, 115111 (2015).

[23] N. E. Bonesteel, I. A. McDonald, and C. Nayak, Phys. Rev. Lett. **77**, 3009 (1996).

[24] C. Nayak and F. Wilczek, Nuclear Physics B **430**, 534 (1994).

[25] C. Nayak and F. Wilczek, Nuclear Physics B **417**, 359 (1994).

[26] E. Fradkin, S. A. Kivelson, M. J. Lawler, J. P. Eisenstein, and A. P. Mackenzie, Annu. Rev. Condens. Matter Phys. **1**, 153 (2010).

[27] J. Rech, C. Pépin, and A. V. Chubukov, Phys. Rev. B **74**, 195126 (2006).

[28] S.-S. Lee, Phys. Rev. B **80**, 165102 (2009).

[29] S. Lederer, Y. Schattner, E. Berg, and S. A. Kivelson, Phys. Rev. Lett. **114**, 097001 (2015).

[30] Y. Schattner, S. Lederer, S. A. Kivelson, and E. Berg, Phys. Rev. X **6**, 031028 (2016).

[31] R. Mahajan, D. M. Ramirez, S. Kachru, and S. Raghu, Phys. Rev. B **88**, 115116 (2013).

[32] E.-G. Moon and A. Chubukov, Journal of Low Temperature Physics **161**, 263 (2010).

[33] J. A. Hertz, Phys. Rev. B **14**, 1165 (1976).

[34] A. J. Millis, Phys. Rev. B **48**, 7183 (1993).

[35] V. Oganesyan, S. A. Kivelson, and E. Fradkin, Phys. Rev. B **64**, 195109 (2001).

[36] D. L. Maslov and A. V. Chubukov, Phys. Rev. B **81**, 045110 (2010).

[37] A. Klein, S. Lederer, D. Chowdhury, E. Berg, and A. Chubukov, Phys. Rev. B **97**, 155115 (2018).

[38] A. Abanov, A. V. Chubukov, and M. R. Norman, Phys. Rev. B **78**, 220507 (2008).

[39] A. J. Millis, S. Sachdev, and C. M. Varma, Phys. Rev. B **37**, 4975 (1988).

[40] A. Abrikosov and L. Gorkov, Sov. Phys. JETP **8**, 1090 (1959).

[41] A. Abrikosov, L. Gorkov, and I. Dzyaloshinski, *Methods of Quantum Field Theory in Statistical Physics*, Dover Books on Physics Series (Dover Publications, 1975).

[42] The numerical factor in Eq. (8) is somewhat different from that in references 11 and 43. This is a consequence of the fact that we used the $T = 0$ expression for the fermionic self-energy, Eq. (3). A more accurate calculation, incorporating the self-energy at $T = T_c$, yields $2\pi T_c = 7.9\omega_0$.

[43] A. V. C. Yiming Wu, Artem Abanov, In preparation (2018).

[44] "See supplemental material for detailed derivations.".